Comparison of Ultrastructure, ECM, and Drug Susceptibility in *M. avium* Biofilms

William R. McManus and Jeffrey S. Schorey *

Posted Date: 19 September 2023

doi: 10.20944/preprints202309.1215.v1

Keywords: Mycobacterium avium; biofilm; resistance; extracellular matrix

Article

Comparison of Ultrastructure, ECM, and Drug Susceptibility in *M. avium* Biofilms

William R. McManus [1] and Jeffrey S. Schorey [2,*]

[1] Department of Biological Sciences, Galvin Life Science Center, University of Notre Dame, Notre Dame, Indiana 46556, USA; wmcmanus@nd.edu
[2] Department of Biological Sciences, Galvin Life Science Center, University of Notre Dame, Notre Dame, Indiana 46556, USA; jeffrey.s.schorey.1@nd.edu
* Correspondence: jeffrey.s.schorey.1@nd.edu

Abstract: Pulmonary infections with *Mycobacterium avium* occur in susceptible individuals following exposure to the bacterium in the environment, where it often persists in biofilms. Many methods have been used to generate biofilms of *M. avium*, and it is unknown whether different approaches generate similar structures and cell phenotypes. To make a parallel comparison of in vitro biofilm ultrastructure, extracellular matrix (ECM) composition, and drug susceptibility of biofilm resident bacteria, we used two published methods to generate *M. avium* biofilms: four week incubation in M63 medium or 24 hour exposure to dithiothreitol (DTT). Scanning electron microscopy revealed differences in biofilm ultrastructure between the two methods, including variation in appearance of ECM materials and morphology of resident cells, while light microscopy and staining with calcofluor white indicated that both biofilms contained polysaccharides characteristic of cellulose. Measuring susceptibility of biofilms to degradation by enzymes suggested differences in structurally important ECM molecules, with DTT biofilms having important protein and, to a lesser extent, cellulose components, and M63 biofilms having moderate protein, cellulose, and DNA components. Both biofilms conferred resistance to the bactericidal effects of amikacin and clarithromycin, with resident cells being killed at >10-fold lower rates than planktonic cells at almost all concentrations. Though these comparisons indicate differences in biofilm responses by *M. avium* under differing conditions, they also suggest common features of biofilm formation including cellulose production and antimicrobial resistance.

Keywords: *Mycobacterium avium*; biofilm; resistance; extracellular matrix

1. Introduction

Mycobacterium avium subs. *hominissuis* is an opportunistic pathogen, causing pulmonary infections in people whose respiratory systems that have been damaged due to injuries or diseases such as cystic fibrosis, bronchiectasis, chronic obstructive pulmonary disease, or emphysema, people who are immunocompromised, and, increasingly, in elderly people without predisposing conditions, especially elderly women with slender physique [1]. Infections with *M. avium* occur worldwide, and increasing incidence has been reported in resource rich countries where longitudinal epidemiological studies have been possible [2–4]. Like many other species of nontuberculous mycobacteria (NTM), *M. avium* is commonly found in numerous natural and engineered habitats, including marginal niches where few species are able to survive [5]. These include household reservoirs, such as showerheads, hot tubs, and humidifiers, that place people in frequent contact with *M. avium* and which have been shown to provide a route for infection via inhalation of aerosols [6–10]. *M. avium* is able to persist in plumbing systems and other habitats by biofilm formation, a process in which the exceptionally hydrophobic mycobacterial cells preferentially adhere to a surface or to particles in suspension, then undergo sessile growth and secrete an extracellular matrix (ECM) [11]. Growth of *M. avium* in biofilms has been observed to cause increased resistance of the bacterium to water treatment applications [12], disinfectants [13,14], and antimicrobial drugs [15,16]. These resistance phenotypes have led to the hypothesis that biofilm growth might condition *M. avium* to succeed as

 doi:10.20944/preprints202309.1215.v1

an opportunistic pathogen and/or that biofilm growth in vivo might explain the recalcitrance of *M. avium* pulmonary infections to therapy [17].

A limitation to our understanding of *M. avium* biofilms is the fact that studies have employed a variety of methods to cause biofilm formation in vitro, and these methods vary in many aspects, including temperature, nutrient and ion availability, substrate material for biofilm attachment, presence or absence of chemical stressors, pH, and presence or absence of flow. Most observations of *M. avium* biofilms have been made using only one method, and this raises uncertainty about whether observations made using one method are characteristic of *M. avium* biofilms broadly or whether they might be caused by conditions specific to that method. A side-by-side comparison of biofilms generated by multiple methods will help delineate which biofilm phenotypes are characteristic of *M. avium* biofilm formation mechanisms generally, and which phenotypes appear in response to specific conditions.

To enable a parallel comparison of *M. avium* biofilms formed in vitro, we selected two previously published methods for producing surface attached biofilms which varied in media composition and time required for biofilm maturation. In the first method, cells of *M. avium* were incubated in a previously described M63-based biofilm medium for 4 weeks to allow biofilm development over an extended period [18–20]. The other method used dithiothreitol (DTT)-induced thiol reductive stress to trigger rapid biofilm development, with biofilm formation occurring in one day [16,21,22]. In this study, we present a comparison of the ultrastructure appearance, biofilm ECM composition, and drug susceptibility of biofilm resident cells of *M. avium* grown in these two biofilm models.

2. Materials and Methods

2.1. Bacterial strains and media

Mycobacterium avium subs. *hominissuis* strains A5 and 2151 were originally isolated from the blood of an AIDS patient with disseminated mycobacterial infection and from the sputum of a patient with pulmonary mycobacterial infection, respectively. These strains were cultured on Middlebrooks 7H10 agar (BD, Franklin Lakes, NJ, USA) containing 10% oleic acid-albumin-dextrose-catalase (OADC; BD, Franklin Lakes, NJ, USA) supplement at 37°C and in Middlebrooks 7H9 broth (BD, Franklin Lakes, NJ, USA) containing 10% OADC at 37°C with constant agitation.

2.2. Biofilm culture conditions

Both biofilm methods studied were adapted for biofilm growth on multiwell polystyrene plates (unless otherwise noted) at 37°C and stationary conditions. Growth of biofilms in M63 media was based on previous studies [18,19]. *M. avium* strains were grown in liquid culture to an optical density 600 nm (OD600) of approximately 0.8, then pelleted and resuspended in biofilm media to an OD600 = 0.2. The biofilm medium consisted of M63 medium (United States Biological, Salem, MA, USA) supplemented with 2% glucose, 0.5% Casamino Acids, 1 mM MgSO4, and 0.7 mM CaCl2. An appropriate volume (1 ml in a 24-well plate well, or equivalent scaled to the surface area of the bottom of other vessels) was dispensed into polystyrene plates, and plates were sealed with parafilm and incubated at 37°C for four weeks. PBS was added to interwell spaces to prevent evaporation. Biofilm formation using dithiothreitol (DTT) was based on previous studies [17,21]. *M. avium* strains were grown in liquid culture to OD600 of approximately 0.8, then pelleted and resuspended in 7H9 broth + 5% OADC to an OD600 = 0.8. DTT (Roche, Basel, Switzerland) was added to a final concentration of 6 mM. An appropriate volume (1 ml in a 24-well plate well, or equivalent) was dispensed into polystyrene plates, and plates were incubated at 37°C for 24 hours.

2.3. Scanning electron microscopy

Biofilms were grown as described above, with the addition of circular glass coverslips to the bottom of the multiwell plate wells. Following biofilm formation, the biofilm media supernatants were removed and the biofilms were rinsed with water. Coverslips with adherent biofilms were removed from the multiwell plates, and the samples were dried overnight. Planktonic samples were

prepared by resuspending *M. avium* grown in liquid culture in PBS, then allowing the bacterial suspension to dry on circular coverslips overnight. Then, the samples were fixed with 2% glutaraldehyde in 0.1 M sodium cacodylate (pH 7.5) for 1 hour. Samples were then rinsed with 0.1 M sodium cacodylate (pH 7.5), fixed in 1% osmium tetroxide, then rinsed again three times with buffer. The samples were then dehydrated using a graded ethanol series, before drying with a critical-point dryer. The dried samples were mounted on SEM stubs and sputter coated with iridium to a thickness of 5μm. Samples were imaged at the Notre Dame Integrated Imaging Facility using a Magellan 400 XHR scanning electron microscope (FEI, Hillsboro, OR, USA).

2.4. Calcofuor white staining

Biofilms were grown as described above, with volumes adjusted for 4-well chamber slides. Bacteria grown in liquid culture, then resuspended in PBS were added to 4-well chamber slides and allowed to dry in the wells overnight. Biofilm media supernatants were removed and the biofilms were rinsed with PBS, then all samples were fixed in 10% formalin for 1 hour. Then they were rinsed three times with PBS, followed by staining with calcofluor white (3 μg/ml; Sigma Aldrich, St. Louis, MO, USA) for 30 minutes. Samples were rinsed again, stained with Auramine M (BD, Franklin Lakes, NJ, USA) for 15 minutes, then destained with acid alcohol and rinsed with water. Finally, samples were mounted using mounting media (Thermo Fisher, Waltham, MA, USA) and imaged using an inverted fluorescent microscope (Zeiss, Oberkochen, Germany).

2.5. Biofilm enzymatic degradation assay

Biofilms were grown in 24-well polystyrene dishes, as described above. Biofilm media supernatants were removed and the biofilms were rinsed with phosphate-buffered saline (PBS). Then enzyme reaction buffers with or without enzymes were added to biofilm containing wells in triplicate, and the biofilms were incubated at 37°C for 6 hours. Enzymes and buffers were formulated as follows: 0.1 mg/ml proteinase K (VWR, Radnor, PA, USA) in 30mM Tris-HCl (pH 8.0), 1 mg/ml Cellulysin Cellulase (MilliporeSigma, Burlington, MA, USA) in 50mM citrate buffer (pH 4.0), and 10 U/ml DNase I (Roche, Basel, Switzerland) in 200 mM Tris-HCl (pH 8.4), 20 mM $MgCl_2$, 500 mM KCl. Following incubation, the enzyme or buffer supernatants were removed from the biofilms, and the biofilms were stained with 0.1% crystal violet for 10 minutes, rinsed twice with water, then allowed to dry overnight. To quantify the residual biomass, the crystal violet was solubilized in 30% acetic acid for 10 minutes with agitation and quantified by measuring the OD600 of the solution.

2.6. Antimicrobial susceptibility

Biofilms were grown as described above, with volumes adjusted for 48-well polystyrene plates. Planktonic cultures were inoculated in normal growth media at an OD600 = 0.1. Amikacin (Alfa Aesar, Haverhill, MA, USA) or clarithromycin (Sigma Aldrich, St. Louis, MO, USA) dilutions were prepared in the growth media corresponding to the different growth conditions (7H9 or M63), applied to the biofilm or planktonic bacteria, then incubated for 4 days at 37°C. Then the culture supernatants were removed, samples were resuspended in PBS, and biofilms were disrupted by scraping and pipetting in PBS+0.5% Tween 80, and a 30 minute incubation in a sonic bath (Thermo Fisher, Waltham, MA, USA). Serial dilutions of bacteria were made in PBS and plated on 7H10 agar +10% OADC to quantify colony forming units (CFU) surviving. Colonies were counted after 10 days of incubation at 37°C.

3. Results

3.1. Biofilm models display differences in ultrastructure cell

The general ultrastructure appearance of biofilms formed by each in vitro method were observed using scanning electron microscopy. Biofilms and planktonic samples of two strains of *M. avium* (A5 and 2151) were included in each comparison to observed strain-specific effects. The strains

 doi:10.20944/preprints202309.1215.v1

in this study represent different serovariants, each expressing a distinct serotype specific glycopeptidolipid (GPL): A5 is a serotype 4 strain and 2151 is a serotype 2 strain. The different methods of in vitro biofilm formation resulted in biofilms with distinct ultrastructure appearances that were similar between strains within a given method (Figure 1). Induction of biofilm formation with DTT gave rise to biofilms with relatively homogenous appearances, with few bacteria visible under a blanket of extracellular material. In contrast, biofilm formation in M63 medium resulted in biofilms with heterogeneous extracellular material appearing as sheets, threads, and granules and the many visible cells had heterogeneous morphologies including elongation and branching (Figure 1).

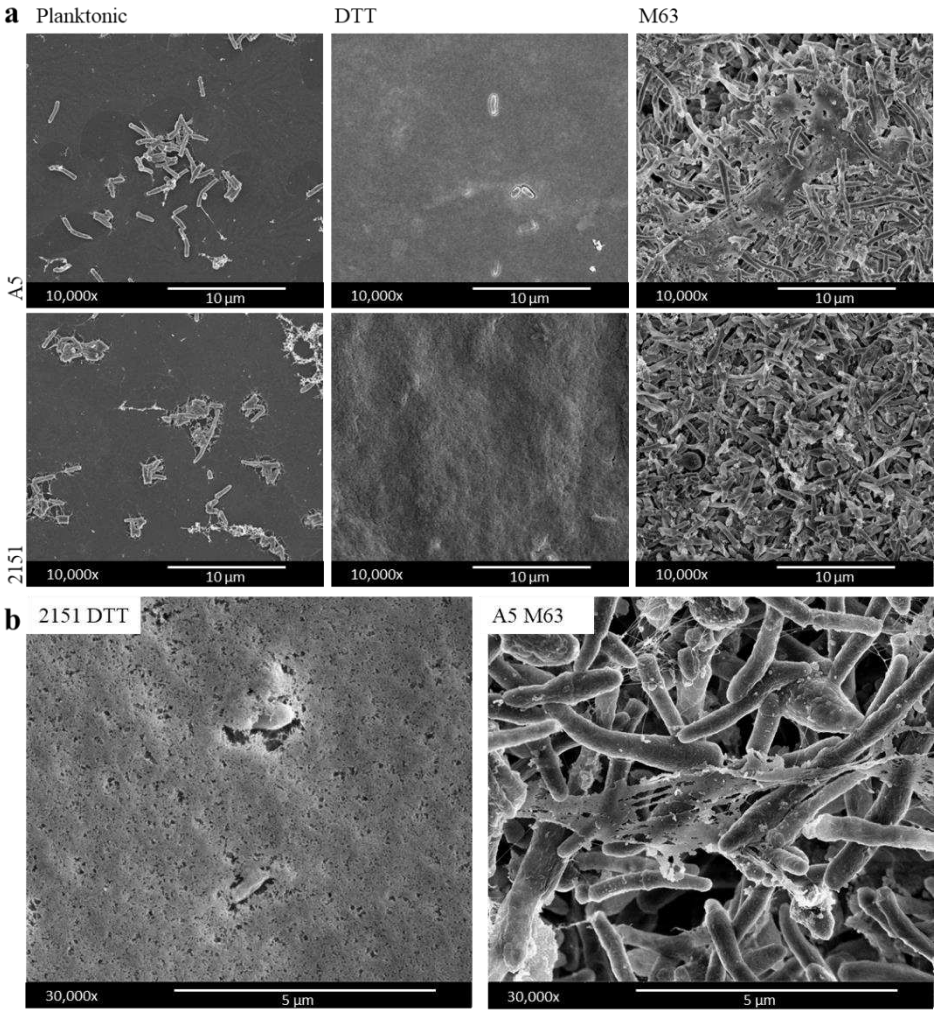

Figure 1. Ultrastructure appearance differs between DTT and M63 *M. avium* biofilm models. SEM was carried out on *M. avium* planktonic or biofilm samples grown on glass coverslips. (**a**) Representative images for each biofilm and planktonic condition for each *M. avium* strain at 10,000X magnification. (**b**) 30,000X magnification showing ECM detail of select representative images from each biofilm model.

3.2. Calcofluor white staining suggests the presence of cellulose in biofilm ECM in both models

Previous studies characterizing the DTT induced biofilm model (Chakraborty et al., 2021) demonstrated the presence of cellulose in that model with multiple mycobacterial species, including *M. avium*. Cellulose was also identified by one study in the ECM of *M. smegmatis* biofilms formed in M63 media (Van Wyk et al., 2017). To compare the presence of polysaccharides with β(1→4) linked D-glucose units (characteristic of cellulose) in specimens from both biofilm models and planktonic bacteria, samples were stained with calcofluor white and counterstained with Auramine M to

Preprints (www.preprints.org) | NOT PEER-REVIEWED | Posted: 19 September 2023 doi:10.20944/preprints202309.1215.v1

visualize the mycobacterial cell membrane. Relative to the planktonic bacteria controls, where no calcofluor white staining was detected, increased staining was observed in both biofilm models for each strain (Figure 2). In the DTT biofilm model, biofilms of *M. avium* strain A5 seemed to stain more strongly than strain 2151, suggesting possible strain specific differences in biofilm ECM composition. In all biofilm samples, calcofluor white staining colocalized closely with the Auramine M mycobacterial cell wall stain.

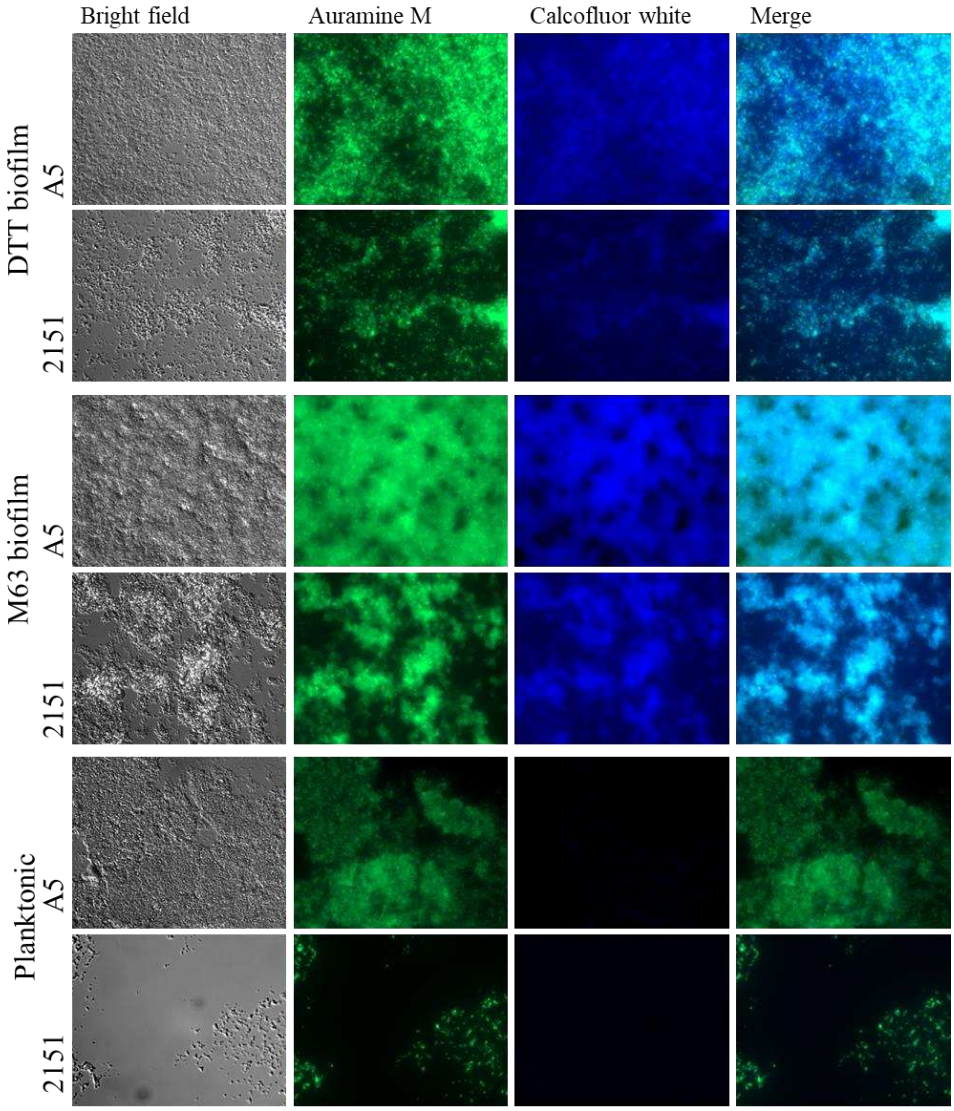

Figure 2. DTT and M63 biofilms both contain cellulose like polysaccharides. Biofilm or planktonic specimens of two *M. avium* strains (A5 and 2151) were grown and fixed in chamber slides, then stained with calcofluor white (3 μg/ml) to detect the β(1→4) linked D-glucose polysaccharides. Samples were then rinsed and stained with Auramine M for detection of the mycobacterial cell envelope, then destained with acid alcohol and rinsed with water. Representative images are shown, visualized at 1000X magnification on a Zeiss inverted fluorescence microscope.

3.3. Biofilm models differ in structurally important ECM molecules

To further compare characteristics of the ECM in each biofilm model, we sought to infer structurally important ECM molecules by exposing biofilms to DNase I, Proteinase K, and Cellulase to cause targeted degradation of ECM molecules that have been identified in previous studies (Rose et al., 2015; Chakraborty et al., 2021). In each biofilm model, the two *M. avium* strains assayed displayed similar patterns of susceptibility to degradation by the different enzymes, suggesting that the structurally important ECM molecules are similar between strains within a given model (Figure

Preprints (www.preprints.org) | NOT PEER-REVIEWED | Posted: 19 September 2023 doi:10.20944/preprints202309.1215.v1

3). Biofilms generated using the DTT model were significantly degraded by Proteinase K, resulting in 87.3% and 92.2% reductions in biomass in strains A5 and 2151, respectively. Degradation by Cellulase was moderate, though variable between replicates, resulting in 45% and 38% reductions in biomass in strains A5 and 2151, respectively. DNase caused no degradation in DTT biofilms of strain 2151 biofilms, and a slight (7%) reduction in biomass in DTT biofilms of strain A5 (Figure 3). Biofilms grown in M63 biofilm media were moderately susceptible to degradation by each enzyme tested, suggesting heterogenous ECM composition, and biofilms of strain A5 exhibited higher degradation by each enzyme than biofilms of strain 2151. For strain A5 and 2151 biofilms, DNase caused biomass reductions of 42% and 18%, Proteinase K caused biomass reductions of 34% and 19%, and Cellulase caused biomass reductions of 40% and 24%, respectively (Figure 3).

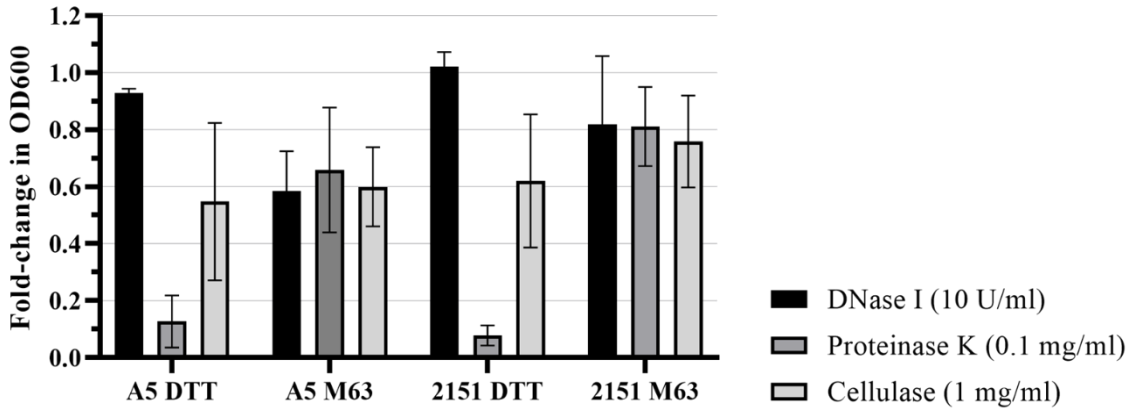

Figure 3. M63 and DTT biofilms have differing susceptibility to enzyme degradation. Biofilms were treated with enzymes or enzyme reaction buffer for 6 hours, then stained for 10 minutes with 0.1% crystal violet, and rinsed twice with water. The stained biomass was dried overnight, then the crystal violet was solubilized in 30% acetic acid and the OD600 was quantified. Fold-change in biofilm biomass was calculated as the ratio of enzyme treated biofilm to paired buffer treated biofilm crystal violet staining, and the plot shows the average and standard deviation of 3-4 biological replicates. Statistics: one sample t-test comparing enzyme treated biofilms to respective buffer treated controls: * $p<0.05$, *** $p<0.001$. .

3.4. Biofilm resident M. avium is resistant to killing by antimicrobial drugs

To assess resistance to killing by two drugs commonly prescribed to treat *M. avium* pulmonary disease, clarithromycin and amikacin, we exposed intact biofilms or planktonic cultures of both strains of *M. avium* to a range of concentrations of each drug for four days. In both strains, each biofilm model increased resistance of bacteria to killing by either drug (Figure 4). Amikacin killed >90% of planktonic *M. avium* A5 at 8 μg/ml and >99% at 32 μg/ml. Planktonic *M. avium* 2151 was more sensitive to killing by amikacin, with >90% killed at 2 μg/ml, >99% killed at 8 μg/ml, and >99.9% killed at 64 μg/ml. In contrast, when bacteria were grown in DTT biofilms both strains required 32x higher concentrations of amikacin (256 μg/ml in A5 and 64 μg/ml in 2151) for >90% killing, and in neither strain were >99% of bacteria killed even at the highest drug concentration tested (512 μg/ml) (Figure 4a). Resistance to killing was even higher in M63 biofilms, where the highest concentration of amikacin (512 μg/ml) did not kill >90% of *M. avium* of either strain in M63 biofilms (Figure 4a). Resistance to clarithromycin in both biofilm models followed a similar pattern. In both strains, clarithromycin killed >90% of planktonic bacteria at 1 μg/ml and >99% at 8 μg/ml (Figure 4b). However, in both biofilm models, the drug failed to kill 90% of bacteria of either strain at any concentration tested, with one exception. In the 2151 DTT biofilm >90% of bacteria were killed at a clarithromycin concentration of 128 μg/ml; however, this is likely not a true indication of drug susceptibility, as clarithromycin failed to kill >90% at drug higher concentrations tested (256 μg/ml and 512 μg/ml) (Figure 4b). An alternative explanation for this observation could be decreased

Preprints (www.preprints.org) | NOT PEER-REVIEWED | Posted: 19 September 2023 doi:10.20944/preprints202309.1215.v1

solubility of the drug at higher concentrations, though evidence of this was not seen in the other clarithromycin treated samples.

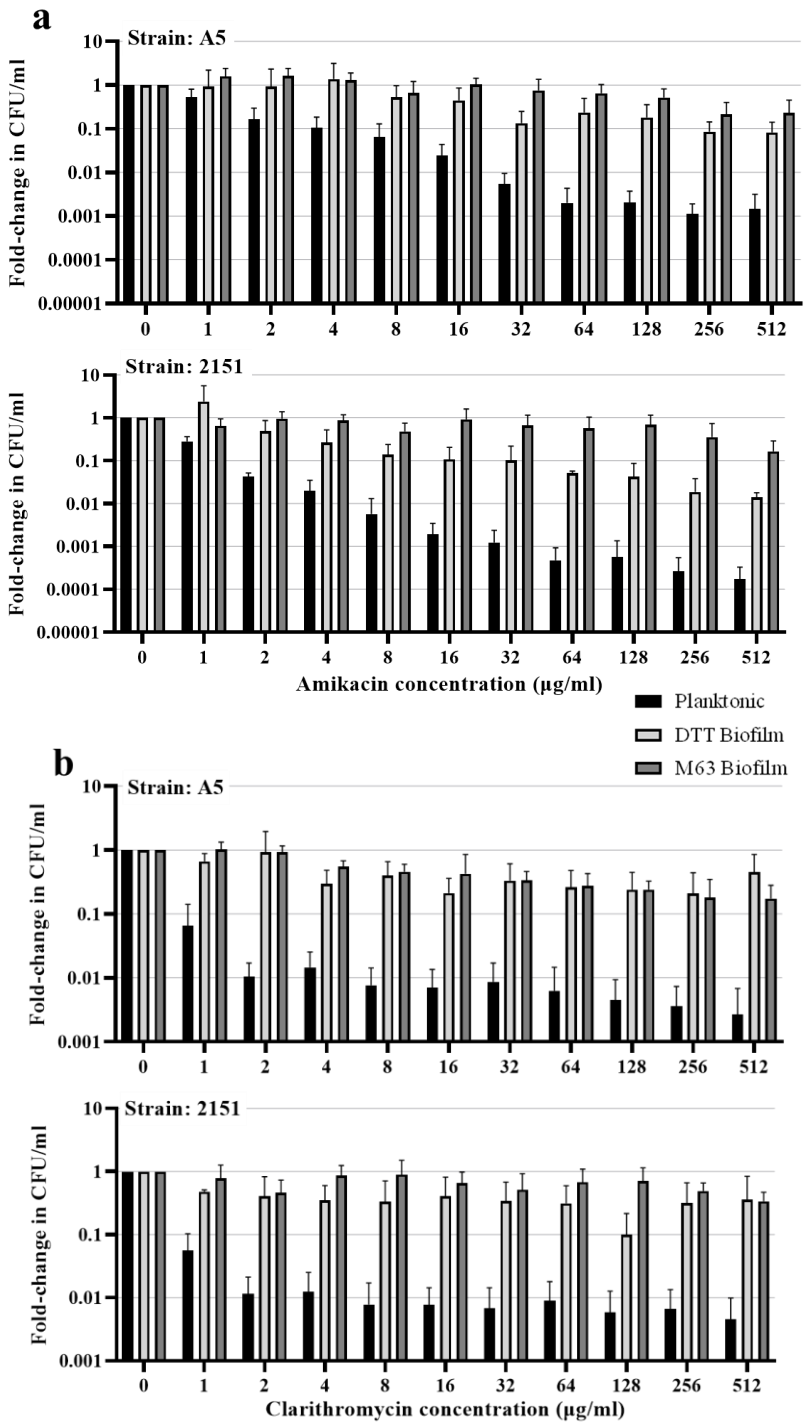

Figure 4. Growth of *M. avium* in biofilms confers resistance to antimycobacterial drugs. *M. avium* strains A5 and 2151 grown in planktonic culture, DTT biofilm, or M63 biofilm were exposed to varying concentrations of **(a)** amikacin or (**b**) clarithromycin for 4 days. After 4 days, supernatants were removed and biofilms were disrupted by scraping, pipetting, and vortexing, and dilutions of each sample were plated on 7H10 agar +10% OADC to quantify CFU. For each condition, counts were normalized to the untreated (0µg/ml) count. The plot shows average fold-change and standard deviation for 3-4 biological replicates.

 doi:10.20944/preprints202309.1215.v1

4. Discussion

In this study, we compared two methods for growing *M. avium* biofilms in vitro, which cause biofilm formation by markedly different stimuli. The M63 biofilm media, four week incubation method likely models the gradual process of biofilm formation that occurs in the environment [18], while the DTT induced, one day incubation method models conditions the opportunistic pathogen might encounter in a potential host [16,21,22]. These methods resulted in biofilms with apparent ultrastructure differences, as observed by SEM. Similar to SEM observations of DTT induced biofilms of *M. tuberculosis* [21], the DTT induced biofilms of both strains of *M. avium* were characterized by an homogenous extracellular matrix concealing the cells within the biofilm. In contrast, the M63 incubated biofilms had extracellular materials with a variety of appearances and many visible cells with variable phenotypes, including elongation and branching. This heterogenous ultrastructure appearance has similarities to previous imaging of *M. avium* biofilms grown with similarly extended incubation times [23,24]. Observation of abnormal bacterial cell morphologies raises the possibility that aberrations from the normal cell division processes may occur when *M. avium* resides in a biofilm for weeks or months. Previous studies in *M. smegmatis* observed that both depletion and overexpression of the tubulin-like protein FtsZ, which is responsible for septum formation in mycobacteria, results in cells with abnormal elongation and branching phenotypes, and this protein could serve as a starting point for further study into the unusual morphologies observed [25–27].

Consistent with the apparent differences in ultrastructure between models, enzymatic degradation of biofilms with enzymes specific to ECM molecules identified in previous studies indicated differences in structurally important molecules between the models. In particular, the DTT biofilm model resulted in biofilms that were readily degraded by Proteinase K, in agreement with the finding of a previous study in *M. tuberculosis* [21], indicating a structurally essential protein component in the ECM of those biofilms, while M63 biofilms were degraded more moderately by Proteinase K. Since the presence of albumin in the culture media is necessary for DTT stimulated biofilm formation [22], it is possible that this is the major source of protein in the biofilm ECM in that model. The models also differed in susceptibility to DNase degradation: biofilms formed in M63 media were moderately degraded by DNase (with strain A5 biofilms degraded to a larger extent that strain 2151 biofilms), while biofilms formed by DTT stimulation had little to no susceptibility to degradation by the enzyme, consistent with previous characterization of the DTT biofilm model in *M. tuberculosis* [21]. Previously, contribution of extracellular DNA (eDNA) to the *M. avium* biofilm ECM was characterized in studies using a biofilm model based on a seven day incubation of bacteria in Hank's Balanced Salt Solution [23,28], where the authors observed strain specific differences in abundance of extracellular DNA produced by *M. avium*, with strain A5 producing more eDNA than the other strains studied, in agreement with our observation that strain A5 M63 biofilms had greater susceptibility to DNase I degradation than strain 2151 M63 biofilms.

Notable similarities were also observed in our comparison of the biofilm ECM in the two models studied. Staining for β(1→4) linked D-glucose polysaccharides with calcofluor white suggested that both biofilm models produced biofilms with cellulose content in the ECM. Taken with the observation of moderate biofilm degradation by Cellulase in both models, these findings suggest that production of cellulose may be a biofilm formation behavior employed by *M. avium* generally. In our study, we observed more modest degradation of the DTT biofilm by cellulase than a previous study [21], where DTT biofilms of *M. tuberculosis* were almost totally disrupted by the enzyme, possibly indicating species specific differences between *M. avium* and *M. tuberculosis*. Production of cellulose by *M. avium* and mycobacteria more broadly was discovered only recently [21], and the genetic basis for this capability is unknown, as mycobacteria lack the classical cellulose synthase gene found in most bacteria [20,29]. In addition to cellulose in the mycobacterial biofilm ECM, *M. tuberculosis* has been observed to produce cellulose in the context of pulmonary infection [16]. Intriguingly, a recent study characterized a glycoside hydrolase family 6 (GH6) cellulase enzyme in *M. smegmatis* with high amino acid similarity to the *M. tuberculosis* cellulase CelA (88% similarity) and to a *M. avium* GH6 enzyme (82% similarity) [20]. In that study, the cellulase enzyme was not used by *M. smegmatis* for metabolism of cellulose, as is the case in other cellulolytic bacteria, but was found to prevent biofilm

formation when overexpressed and to disrupt the biofilm ECM of the bacterium when added exogenously. This suggests the possibility that this cellulase could have a functional role in biofilm modeling by reverting bacteria in a biofilm back into the planktonic state, similar to a behavior observed previously in the cellulolytic bacterium *Acetivibrio thermocellus* [20,30]. Our observation of cellulose in biofilms formed by *M. avium* in response to different stimuli adds further motivation to fully characterize the mechanism of cellulose production in mycobacteria, the stimuli that trigger cellulose production, the role of mycobacterial cellulase enzymes, and the relevance of these processes for both biofilm and in vivo persistence.

The biofilm models were also similar in their conferral of resistance to killing by clarithromycin and amikacin. Cells residing in either biofilm model were killed at >10-fold lower rates than planktonic cells at almost all concentrations tested. This is in general agreement with other studies of each model, where increased resistance has been observed previously: *M. avium* and other NTM in DTT induced biofilms have been shown to be resistant to bedaquiline [16], and cells of *M. smegmatis* grown in M63 biofilms have been shown to have increased resistance to rifampin [20]. There are multiple potential explanations for the resistance observed in each model, and the differences in media and incubation time likely lead to some differences between models in the mechanisms contributing. However, it is possible that, despite the differences in the models, there may be common mechanisms of increased resistance in biofilm resident *M. avium*. Studies of *M. avium* grown in other models have demonstrated that bacteria grown in biofilms initially retain high levels of resistance to killing by antimicrobial drugs and disinfectants when resuspended, then lose resistance after 24 hours of growth in liquid culture, suggesting that changes in gene expression play a role in resistance [13,31]. Therefore, future studies comparing overall gene expression of bacteria residing in different biofilm models may offer leads toward discovering adaptations in gene expression leading to resistance that are common to *M. avium* biofilms formed under differing conditions.

The design of this study, in which we compared aspects of *M. avium* biofilm appearance, ECM composition, and resident cell phenotypes between two biofilm models, should serve as a template for expanded parallel analyses that could include additional biofilm models and employ additional methods to characterize the biofilms and their constituent cells. Characterization and comparison of the involvement of membrane lipids in *M. avium* biofilms would be particularly informative, as studies of these molecules in the context of biofilms have been carried out almost entirely in other mycobacterial species. For instance, *M. tuberculosis* and *M. smegmatis* pellicle (liquid-air interface) biofilms contain short chain mycolic acids in the ECM [32–35], and these have not been assayed in biofilms of other species. Additionally, *M. avium* and several other NTM express glycopeptidolipids (GPLs) which are necessary for biofilm formation [18,19,36], may have altered expression under biofilm conditions [37], and also appear to be immunologically important in the context of exposure and infection [38]. Further characterization of the GPL content and localization in *M. avium* biofilms is necessary to determine the specific role that these molecules play in biofilm formation.

Author Contributions: W.R.M. and J.S.S contributed to conceptualization and methodology. W.R.M. carried out the experiments, analyses, and data visualization. W.R.M. prepared the original draft of the manuscript and carried out revisions under the critical guidance of J.S.S. J.S.S. was responsible for supervision, project administration, and funding acquisition. Both authors have read and agreed to the published version of the manuscript.

Funding: JSS is funded by National Institute of Heath, grant number R21 AI168662

Institutional Review Board Statement: N/A

Data Availability Statement: Data from this study can be found as part of the manuscript.

Acknowledgments: We are grateful for the technical expertise and guidance from members of the University of Notre Dame Integrated Imaging Facility, especially Sarah Chapman and Tatyana Orlova. We are also grateful to Felipe Santiago Tirado and Ana Flores Mireles for use of their Zeiss inverted fluorescent microscope.

Conflicts of Interest: The authors declare no conflict of interest.

References

1. Chalmers, J.D.; Aksamit, T.; Carvalho, A.C.C.; Rendon, A.; Franco, I. Non-Tuberculous Mycobacterial Pulmonary Infections. *Pulmonology*, **2018**, *24*, 120–131.
2. Hoefsloot, W.; Van Ingen, J.; Andrejak, C.; Ängeby, K.; Bauriaud, R.; Bemer, P.; Beylis, N.; Boeree, M.J.; Cacho, J.; Chihota, V.; Chimara, E.; Churchyard, G.; Cias, R.; Daza, R.; Daley, C.L.; Dekhuijzen, P.N.R.; Domingo, D.; Drobniewski, F.; Esteban, J.; Fauville-Dufaux, M.; Folkvardsen, D.B.; Gibbons, N.; Gómez-Mampaso, E.; Gonzalez, R.; Hoffmann, H.; Hsueh, P.R.; Indra, A.; Jagielski, T.; Jamieson, F.; Jankovic, M.; Jong, E.; Keane, J.; Koh, W.J.; Lange, B.; Leao, S.; Macedo, R.; Mannsåker, T.; Marras, T.K.; Maugein, J.; Milburn, H.J.; Mlinkó, T.; Morcillo, N.; Morimoto, K.; Papaventsis, D.; Palenque, E.; Paez-Peña, M.; Piersimoni, C.; Polanová, M.; Rastogi, N.; Richter, E.; Ruiz-Serrano, M.J.; Silva, A.; Da Silva, M.P.; Simsek, H.; Van Soolingen, D.; Szabó, N.; Thomson, R.; Fernandez, T.T.; Tortoli, E.; Totten, S.E.; Tyrrell, G.; Vasankari, T.; Villar, M.; Walkiewicz, R.; Winthrop, K.L.; Wagner, D. The Geographic Diversity of Nontuberculous Mycobacteria Isolated from Pulmonary Samples: An NTM-NET Collaborative Study. *Eur. Respir. J.*, **2013**, *42*, 1604–1613, 10.1183/09031936.00149212.
3. Sharma, S.; Upadhyay, V. Epidemiology, Diagnosis & Treatment of Non-Tuberculous Mycobacterial Diseases. *Indian Journal of Medical Research*, **2020**, *152*, 185–226.
4. Prevots, D.R.; Marras, T.K. Epidemiology of Human Pulmonary Infection with Nontuberculous Mycobacteria a Review. *Clinics in Chest Medicine*, **2015**, *36*, 13–34.
5. Falkinham, III, J.O. Surrounded by Mycobacteria: Nontuberculous Mycobacteria in the Human Environment. *J. Appl. Microbiol.*, **2009**, *107*, 356–367, 10.1111/j.1365-2672.2009.04161.x.
6. Tzou, C.L.; Dirac, M.A.; Becker, A.L.; Beck, N.K.; Weigel, K.M.; Meschke, J.S.; Cangelosi, G.A. Association between Mycobacterium Avium Complex Pulmonary Disease and Mycobacteria in Home Water and Soil a Case-Control Study. *Ann. Am. Thorac. Soc.*, **2020**, *17*, 57–62, 10.1513/AnnalsATS.201812-915OC.
7. Falkinham, J.O.; Iseman, M.D.; de Haas, P.; van Soolingen, D. Mycobacterium Avium in a Shower Linked to Pulmonary Disease. *J. Water Health*, **2008**, *6*, 209–213, 10.2166/wh.2008.032.
8. Mangione, E.J.; Huitt, G.; Lenaway, D.; Beebe, J.; Bailey, A.; Figoski, M.; Rau, M.P.; Albrecht, K.D.; Yakrus, M.A. Nontuberculous Mycobacterial Disease Following Hot Tub Exposure. *Emerg. Infect. Dis.*, **2001**, *7*, 1039–1042, 10.3201/EID0706.010623.
9. Nishiuchi, Y.; Maekura, R.; Kitada, S.; Tamaru, A.; Taguri, T.; Kira, Y.; Hiraga, T.; Hirotani, A.; Yoshimura, K.; Miki, M.; Ito, M. The Recovery of Mycobacterium Avium-Intracellulare Complex (MAC) from the Residential Bathrooms of Patients with Pulmonary MAC. *Clin. Infect. Dis.*, **2007**, *45*, 347–351, 10.1086/519383.
10. Hamilton, L.A.; Falkinham, J.O. Aerosolization of Mycobacterium Avium and Mycobacterium Abscessus from a Household Ultrasonic Humidifier. *J. Med. Microbiol.*, **2018**, *67*, 1491–1495, 10.1099/jmm.0.000822.
. Falkinham, J. Mycobacterium Avium Complex: Adherence as a Way of Life. *AIMS Microbiol.*, **2018**, *4*, 428–438, 10.3934/microbiol.2018.3.428.
11. Norton, C.D.; LeChevallier, M.W.; Falkinham, J.O. Survival of Mycobacterium Avium in a Model Distribution System. *Water Res.*, **2004**, *38*, 1457–1466, 10.1016/j.watres.2003.07.008.
12. Steed, K.A.; Falkinham, J.O. Effect of Growth in Biofilms on Chlorine Susceptibility of Mycobacterium Avium and Mycobacterium Intracellulare. *Appl. Environ. Microbiol.*, **2006**, *72*, 4007–4011, 10.1128/AEM.02573-05.
13. Carter, G.; Wu, M.; Drummond, D.C.; Bermudez, L.E. Characterization of Biofilm Formation by Clinical Isolates of Mycobacterium Avium. *J. Med. Microbiol.*, **2003**, *52*, 747–752, 10.1099/jmm.0.05224-0.
14. Mcnabe, M.; Tennant, R.; Danelishvili, L.; Young, L.; Bermudez, L.E. Mycobacterium Avium Ssp. Hominissuis Biofilm Is Composed of Distinct Phenotypes and Influenced by the Presence of Antimicrobials. *Clin. Microbiol. Infect.*, **2011**, *17*, 697–703, 10.1111/j.1469-0691.2010.03307.x.
15. Chakraborty, P.; Bajeli, S.; Kaushal, D.; Radotra, B.D.; Kumar, A. Biofilm Formation in the Lung Contributes to Virulence and Drug Tolerance of Mycobacterium Tuberculosis. *Nat. Commun.*, **2021**, *12*, 10.1038/s41467-021-21748-6.
16. Chakraborty, P.; Kumar, A. The Extracellular Matrix of Mycobacterial Biofilms: Could We Shorten the Treatment of Mycobacterial Infections? *Microbial Cell*, **2019**, *6*, 105–122.
17. Freeman, R.; Geier, H.; Weigel, K.M.; Do, J.; Ford, T.E.; Cangelosi, G.A. Roles for Cell Wall Glycopeptidolipid in Surface Adherence and Planktonic Dispersal of Mycobacterium Avium. *Appl. Environ. Microbiol.*, **2006**, *72*, 7554–7558, 10.1128/AEM.01633-06.
18. Recht, J.; Kolter, R. Glycopeptidolipid Acetylation Affects Sliding Motility and Biofilm Formation in Mycobacterium Smegmatis. *J. Bacteriol.*, **2001**, *183*, 5718–5724, 10.1128/JB.183.19.5718-5724.2001.
19. Van Wyk, N.; Navarro, D.; Blaise, M.; Berrin, J.-G.; Henrissat, B.; Drancourt, M.; Kremer, L. Characterization of a Mycobacterial Cellulase and Its Impact on Biofilm-and Drug-Induced Cellulose Production. *Glycobiology*, **2017**, *27*, 392–399, 10.1093/glycob/cwx014.
20. Trivedi, A.; Mavi, P.S.; Bhatt, D.; Kumar, A. Thiol Reductive Stress Induces Cellulose-Anchored Biofilm Formation in Mycobacterium Tuberculosis. *Nat. Commun.*, **2016**, *7*, 10.1038/ncomms11392.

21. Mavi, P.S.; Singh, S.; Kumar, A. Media Component Bovine Serum Albumin Facilitates the Formation of Mycobacterial Biofilms in Response to Reductive Stress. *BMC Microbiol.*, **2023**, *23*, 111, 10.1186/s12866-023-02853-6.
22. Rose, S.J.; Babrak, L.M.; Bermudez, L.E. Mycobacterium Avium Possesses Extracellular DNA That Contributes to Biofilm Formation, Structural Integrity, and Tolerance to Antibiotics. *PLoS One*, **2015**, *10*, 10.1371/journal.pone.0128772.
23. Nishiuchi, Y. Ultrastructure of the Mycobacterium Avium Subsp. Hominissuis Biofilm. *Microbes Environ.*, **2021**, *36*, 1–7, 10.1264/jsme2.ME20128.
24. Dziadek, J.; Rutherford, S.A.; Madiraju, M. V.; Atkinson, M.A.L.; Rajagopalan, M. Conditional Expression of Mycobacterium Smegmatis FtsZ, an Essential Cell Division Gene. *Microbiology*, **2003**, *149*, 1593–1603, 10.1099/mic.0.26023-0.
25. Singh, A.K.; Carette, X.; Potluri, L.P.; Sharp, J.D.; Xu, R.; Prisic, S.; Husson, R.N. Investigating Essential Gene Function in Mycobacterium Tuberculosis Using an Efficient CRISPR Interference System. *Nucleic Acids Res.*, **2016**, *44*, 10.1093/nar/gkw625.
26. Hett, E.C.; Rubin, E.J. Bacterial Growth and Cell Division: A Mycobacterial Perspective. *Microbiol. Mol. Biol. Rev.*, **2008**, *72*, 126–156, 10.1128/mmbr.00028-07.
27. Rose, S.J.; Bermudez, L.E. Identification of Bicarbonate as a Trigger and Genes Involved with Extracellular DNA Export in Mycobacterial Biofilms. *MBio*, **2016**, *7*, 10.1128/mBio.01597-16.
28. Römling, U.; Galperin, M.Y. Bacterial Cellulose Biosynthesis: Diversity of Operons, Subunits, Products, and Functions. *Trends in Microbiology*, **2015**, *23*, 545–557.
29. Dumitrache, A.D.; Wolfaardt, G.; Allen, G.; Liss, S.N.; Lynd, L.R. Form and Function of Clostridium Thermocellum Biofilms. *Appl. Environ. Microbiol.*, **2013**, *79*, 231–239, 10.1128/AEM.02563-12.
30. Falkinham, J.O. Growth in Catheter Biofilms and Antibiotic Resistance of Mycobacterium Avium. *J. Med. Microbiol.*, **2007**, *56*, 250–254, 10.1099/jmm.0.46935-0.
31. Ojha, A.; Anand, M.; Bhatt, A.; Kremer, L.; Jacobs, W.R.; Hatfull, G.F. GroEL1: A Dedicated Chaperone Involved in Mycolic Acid Biosynthesis during Biofilm Formation in Mycobacteria. *Cell*, **2005**, *123*, 861–873, 10.1016/j.cell.2005.09.012.
32. Ojha, A.; Hatfull, G.F. The Role of Iron in Mycobacterium Smegmatis Biofilm Formation: The Exochelin Siderophore Is Essential in Limiting Iron Conditions for Biofilm Formation but Not for Planktonic Growth. *Mol. Microbiol.*, **2007**, *66*, 468–483, 10.1111/j.1365-2958.2007.05935.x.
33. Ojha, A.K.; Baughn, A.D.; Sambandan, D.; Hsu, T.; Trivelli, X.; Guerardel, Y.; Alahari, A.; Kremer, L.; Jacobs, W.R.; Hatfull, G.F. Growth of Mycobacterium Tuberculosis Biofilms Containing Free Mycolic Acids and Harbouring Drug-Tolerant Bacteria. *Mol. Microbiol.*, **2008**, *69*, 164–174, 10.1111/j.1365-2958.2008.06274.x.
34. Ojha, A.K.; Trivelli, X.; Guerardel, Y.; Kremer, L.; Hatfull, G.F. Enzymatic Hydrolysis of Trehalose Dimycolate Releases Free Mycolic Acids during Mycobacterial Growth in Biofilms. *J. Biol. Chem.*, **2010**, *285*, 17380–17389, 10.1074/jbc.M110.112813.
35. Yamazaki, Y.; Danelishvili, L.; Wu, M.; MacNab, M.; Bermudez, L.E. Mycobacterium Avium Genes Associated with the Ability to Form a Biofilm. *Appl. Environ. Microbiol.*, **2006**, *72*, 819–825, 10.1128/AEM.72.1.819-825.2006.
36. Maya-Hoyos, M.; Leguizamón, J.; Mariño-Ramírez, L.; Soto, C.Y. Sliding Motility, Biofilm Formation, and Glycopeptidolipid Production in Mycobacterium Colombiense Strains. *Biomed Res. Int.*, **2015**, *2015*, 419549, 10.1155/2015/419549.
37. Schorey, J.S.; Sweet, L. The Mycobacterial Glycopeptidolipids: Structure, Function, and Their Role in Pathogenesis. *Glycobiology*, **2008**, *18*, 832–841.